# A Discrete-Time Robust Adaptive Controller Applied to a Bidirectional Isolated Converter

Edivan Laercio Carvalho[1], Rodrigo Varella Tambara[1], Rafael Cardoso[2], Leandro Michels[1]
[1]Universidade Federal de Santa Maria – UFSM, Santa Maria - RS, Brazil
[2]Universidade Tecnológica Federal do Paraná – UTFPR, Pato Branco - PR, Brazil
E-mails: edivan.labensaios@gepoc.ufsm.br, rodvarella@yahoo.com.br, rcardoso@utfpr.edu.br, michels@gepoc.ufsm.br

***Abstract*—The insertion of batteries with low voltage levels and high charge capacity is of great interest for application in microgrids, mainly on assist the regulation of high voltage DC links, used to integrate power generation sources and batteries. The solution for this application are the use of bidirectional converters that operate like as charge/discharge controllers with high voltage gain. In this application, controllers with fixed gains based on average models, cannot guaranteed high performance due the variations on batteries state of charge and disturbances on the DC link loads. A solution are purposed in this work, where are applied an adaptive controller in battery discharge mode, critical case due the necessity to representation the system by small-signal models. Adaptive controllers are interesting because they are not depend directly on such models. Results obtained by simulations demonstrate that this strategy guaranteed robustness and high performance against parametric variations.**

***Key-Words:*** **Adaptive Control, Bidirectional Converters, Battery Charger, Charger Controllers.**

## I. INTRODUCTION

On microgrids, multiple power source, energy storage devices and loads are connected by means of high voltage DC link (300 V – 800 V) used to feed DC-AC converters. In this application, batteries of 12 V to 48 V are used to aid in power dispatch and DC link voltage control [1]. Therefore, energy storage systems, based on DC-DC converters, inverters and battery banks are fundamental for renewable power sources, like a photovoltaic generation and wind turbines, where batteries acts as accumulators or auxiliary sources in periods of high demand of loads or in cases of low generation levels or faults in main sources [1]-[4]. The operation of these systems consists of adequate the voltage of the batteries to levels appropriate to the DC link, making fundamental part of energy storage systems DC-DC converters with high voltage gain. The use of converters in these applications is due to the need to control the charge current of the batteries as well as to regulate the voltage of the DC link in cases of failure of the main source [4], [5].

In relation of charge process, the control design have to anticipate harmful situations, as overcharge, deep discharge or raising of temperature. About the discharge, the main specifications of converter are related with settling time response, due the necessity of maintained constant the voltage on DC link, as well show robustness against changes of loads [4], [6], [7]. Due de several situations involved with the energy storage systems operations, different papers purpose the use of bidirectional isolated converters, specially due the safety of battery bank and due the performance issues as efficiency and high voltage gain [8]-[15]. Many cited works focusses on design and analysis of converter in steady-state, however, the obtaining and verifying of models and transitory analysis of this converters is still an aspect that be better explored, especially in applications that involving battery banks, that showing nonlinear and time-variant dynamics, therefore, complex to be modelling [16]-[20].

The Figure 1 show the circuit purposed by [13] to regulating the DC link voltage on a fixed value, when considering the both operation modes of battery banks – charge and discharge –, however, modeling requires representation by small signal model, making it difficult the obtain robust controllers [16]. Due to closed-loop control are essential for these systems, and design of controllers with fixed gains depend on well-defined models, commonly are adopted for representation of theses converters the approach of average-model on state-space [21]-[22]. However, being dependent on an operating point [23], for applications on energy storage systems becomes limited due the variations on battery state of charge, changes on loads connected on DC link and nonlinearities of converters represented by small-signal models.

To compensate parametric variations of plant, unmodeled dynamics and guaranteed high performance, the application of adaptive controllers are interesting. The implemented of the same can be by means of Least Square or Gradient algorithms, which differ in the way they calculate their adaptation rates [24]. In this work, a Gradient algorithm are used to present a fixed parametric adaptation rate, resulting in greater simplicity of implementation and design, a characteristic of interest for DSP implementation due to the reduced number of computations to be performed. From the power circuit shown in Figure 1, the control design are develop to regulate the voltage of the DC link during the discharge process of the battery bank. Therefore, this work contributes to the development of bidirectional converters, by ensuring the control and regulation of DC link voltage, presenting robustness against load variations and independence of small-signal models.

## II. PROBLEM DESCRIPTION AND SMALL-SIGNAL ANALYSIS

Figure 1 show the circuit purposed by [13] to regulation of DC link voltage in a fixed value on both battery banks operation mode, charge and discharge. Initially, in battery bank side the converter *B* acts like a current-fed converter, raising the voltage of battery bank during the discharge process, case called Boost mode. On DC link side, the converter *A* acts like a step-down converter, on Buck mode, realizing the batteries charge.

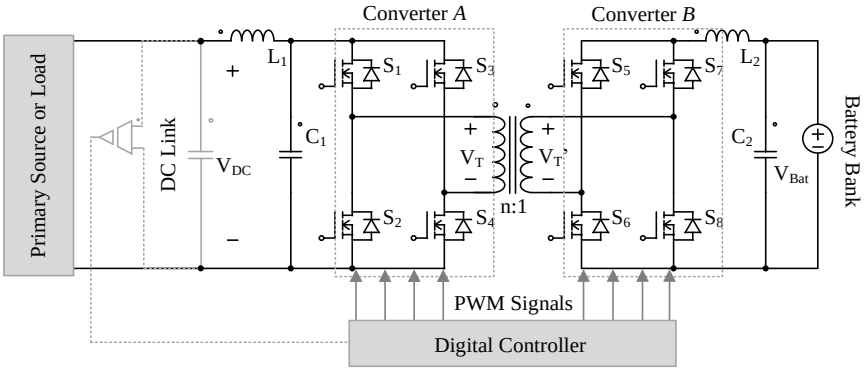


Fig. 1. Power Circuit of Full-Bridge bidirectional converter.

The equivalent circuit showed in Figure 2 can represent converter acts like a voltage step-down.

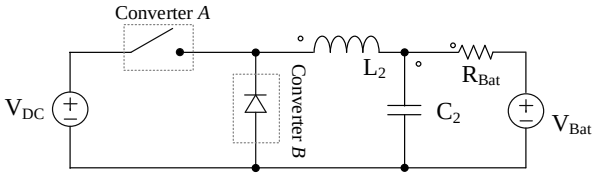


Fig. 2. Equivalent circuit of converter on Buck mode.

For this operation mode, the converter present a linear transfer function, directly dependent of duty cycle (D) of converter, which represents a variable that can be controlled. For verified this statement, [13] presents the static gain, defined by:

$$\frac{V_{Bat}}{V_{DC}} = D\,, \qquad (1)$$

Therefore, the relation between the voltages of the batteries and DC bus in this case, are directly dependent on D.

Due to the possibility of represent this plant by means of a larger-signal model, although considering the variations concerning of the state of charge of the batteries, it is possible to obtain high performance controllers with fixed gains for the charge of batteries. Mainly because the parametric variations related to the charge dynamics of the batteries are, slow and do not require fast transient responses of the charge controllers [16]. To discharge mode, the converter operates according the equivalent circuit in Figure 3.

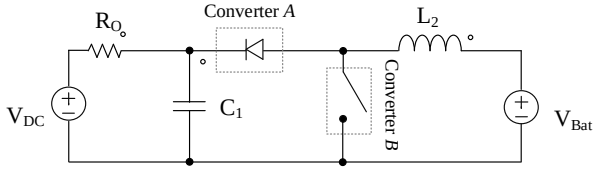


Fig. 3. Equivalent circuit of converter on Boost mode.

In this situation, the bidirectional converter acts raising the battery bank voltage by means the follow equation:

$$\frac{V_{C1}}{V_{Bat}} = \frac{1}{1-D}\,. \qquad (2)$$

Clearly, because the converter transfer function - which must relate the voltages of the battery bank and DC bus - aren't depend directly on the duty cycle, it is not possible to perform a PWM modulation directly, necessary for control design purposes. For this situation, approaches that involve small-signal models are commonly used. This strategy consists in manipulating the converter transfer function in order to obtain a model dependent on a controllable variable, related to perturbations on the duty cycle [23].

Since this is a linearization, small-signal models are only valid for regions near an operating point, under which the system was modeled. Therefore, fixed-gains controllers – designed from these models – cannot guarantee performance and robustness, especially against parametric variations of the plant, or disturbances, such as variations of loads connected on DC link. To investigate this information, in this section, it will be show the development of small-signal model for the converter in Boost mode. The follow analysis presented a reduced order model, characteristic interesting for Robust Model Reference Adaptive Controller – RMRAC – implementation, since it allows reducing the number of interactions necessary to adapt the controller gains. For modeling purposes, the equivalent circuit shown in Figure 3 are be adopted. The Table I presented the circuit parameters.

**TABLE I**
**DETAILS OF DIMENSIONED COMPONENTS**

| Parameters | Specifications |
|---|---|
| DC Link | Nominal voltage: 400 V<br>Power: 1 kW<br>Load ($R_O$): 40 Ω |
| Battery Banks | Nominal Voltage: 48 V (4 x 12V) |
| Transformer | 4:1 |
| Inductor $L_1$ | 0.8 mH |
| Capacitor $C_1$ | 2 µF x 500 V  $\Delta V_{C1}$: 20 V |
| Inductor $L_2$ | 180 µH  $\Delta i_{L2}$: 3.5 A |
| Capacitor $C_2$ | 22 µF x 150 V  $\Delta V_{C2}$: 0.48 V |

The following analysis considers the following assumptions: a) in cases of DC link failure, the $V_{DC}$ voltage must be less than nominal voltage and must be compensating by the battery bank; b) the load connected on DC link results in the nominal power, equal to 1 kW.

### *A. Steady-state analysis and small-signal model*

In Boost mode, the bidirectional converter acts with the objective to regulated the DC link voltage. In this operation mode, converter *B* acts as an inverter transferring the energy stored on batteries to DC link, while the converter *A* acts

like a rectifier, therefore, the equivalent circuit showed in Figure 3 are valid.

**Stage 1 – Figure 4-a, $t_0$-$t_1$:** at first stage of converter operation as voltage step-up, the inductor $L_2$ is demagnetized for the output system while $C_1$ are charged. From the equivalent circuit showing in Figure 4-a, has the following equations: $V_{L2}=V_{Bat}-V_{DC}$ e $i_{C1}=i_{L2}-i_{RO}$.

**Stage 2– Figure 4-b, $t_1$-T:** for the inductor $L_2$ has charged again, the converter B acts interrupting the power flux from batteries to DC link. In this moment $L_2$ are connected in parallel with the batteries, therefore, presenting a positive voltage $V_{L2}= V_{Bat}$, while $C_1$, for not suffering direct interference of the batteries is discharged, with a current equal $i_{C1}=-i_{RO}$.

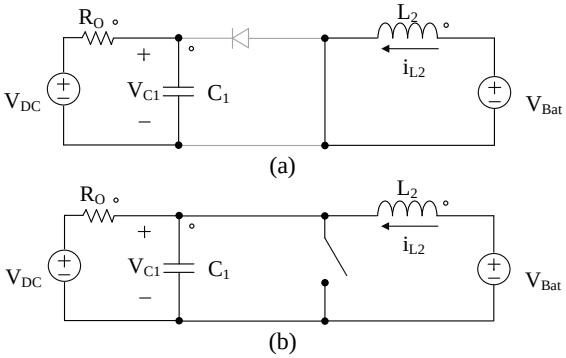


Fig. 4. Equivalent circuits of converter operation on Boost mode.

Considering as state variables $X_1=V_{C1}$, $X_2=i_{L2}$, according to the analysis of the equivalent circuits, the state space that define the converter model are:

$$\begin{cases} A_1 = \begin{bmatrix} -\frac{1}{R_O C_1} & \frac{1}{C_1} \\ -\frac{1}{L_2} & 0 \end{bmatrix}, B_1 = \begin{bmatrix} \frac{V_{DC}}{R_O C_1} \\ \frac{V_{Bat}}{L_2} \end{bmatrix}, \\ A_2 = \begin{bmatrix} -\frac{1}{R_O C_1} & 0 \\ 0 & 0 \end{bmatrix}, B_2 = \begin{bmatrix} \frac{V_{DC}}{R_O C_1} \\ \frac{V_{Bat}}{L_2} \end{bmatrix} \end{cases} \quad (3)$$

where, Stage 1 is represented by the matrices $\mathbf{A}_1$ and $\mathbf{B}_1$, and Stage 2 represented by $\mathbf{A}_2$ and $\mathbf{B}_2$. Being

$$\begin{cases} \mathbf{A} = \mathbf{A}_1 \cdot D + \mathbf{A}_2 \cdot (1-D) \\ \mathbf{B} = \mathbf{B}_1 \cdot D + \mathbf{B}_2 \cdot (1-D) \end{cases}, \quad (4)$$

the average model in state space are given by:

$$\begin{cases} \dot{\mathbf{X}} = \mathbf{A} \cdot \mathbf{X} + \mathbf{B} \cdot u(t) \\ \mathbf{Y} = \mathbf{C} \cdot \mathbf{X} \end{cases}, \quad (5)$$

where the function u(t) represents the energization of the system, and the matrix $\mathbf{C}$ = [1 0]. However, in order to represent the system as a function of the converter duty cycle, it is necessary to perform a mathematical manipulation in the average model in order to represent it as a function of a controllable variable.

The analysis performed in [21] results on the small-signal model. This model are obtained around an operating point, has as input variable d, associated with the manipulation of the converter duty cycle, and therefore suitable for control purposes. The small-signal average model for any converter, is defined by the analysis of perturbations on the state variables of the system when it is in steady state. From this principle, the analysis presents by [21] results on model given by:

$$\begin{aligned} \dot{\hat{\mathbf{x}}} &= \mathbf{A} \cdot \hat{\mathbf{x}} + \mathbf{B}_s \cdot d, \\ \mathbf{y} &= \mathbf{C} \cdot \hat{\mathbf{x}}, \end{aligned} \quad (6)$$

when $\mathbf{B_s}$ is equal to $\mathbf{B_s}=(\mathbf{A_1}-\mathbf{A_2})\cdot(-\mathbf{A}^{-1}\cdot\mathbf{B})+(\mathbf{B_1}-\mathbf{B_2})$, and d represent a perturbation on converter duty cycle, D.

### *B. Verification and analysis of the model*

The analysis of small-signal and average model were performed aiming to represent the system in a similar way to equation (6). In order to verify the validity of the model, simulations were performed using the Matlab and PSIM software, in order to compare the model response with the simulated circuit, involving unmodeled dynamics such as $L_1$, $C_2$, transformer and batteries. To simulate a fault in the DC link, a minimum voltage equal to 300 V was considered, while the $R_O$ load was set to result in the nominal power of the converter, when it is regulated at its rated voltage, therefore $R_O$ = 40 Ω.

Initially, the converter it was test on a region near the nominal voltage of DC link. On steady state are applied a perturbation under the converter duty cycle for resulting in nominal voltage of DC link. The same test are realize on the average model with the objective to compare the model response and the circuit simulation at software PSIM. The result are showed in Figure 5, that verified the validly of model, since both the simulated circuit and the small-signal model show similar response. From the small-signal model in state space, the transfer function is obtain in (7).

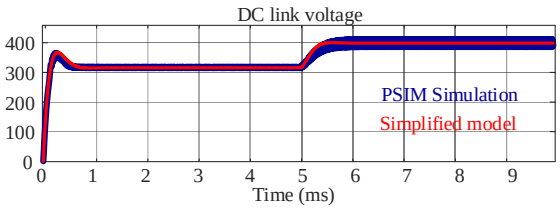


Fig. 5: Comparison between the simulated circuit response and the average models of large and small-signals.

$$G_P(s) = \frac{V_{DC}(s)}{d(s)} = \frac{-1.298 \cdot 10^6 s + 1.33 \cdot 10^{11}}{s^2 + 1.25 \cdot 10^4 s + 6.418 \cdot 10^7}. \quad (7)$$

At a second moment, are realized different tests considering variations on loads connected on DC link. For different power levels are obtained the bode diagram of resulting models, showed in Figure 6, from which it is possible to verify the parametric variations of the plant, which depends directly on the converter operating point.

## III. Design and Structure of Control System

From the models presented on previous section, can be performed the design of control system. Based on the

structure showed in Figure 1, the control system are implemented.

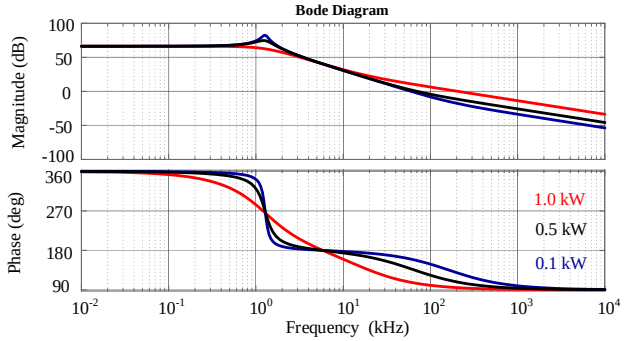


Fig. 6: Bode diagrams for different power levels.

Due the uncertainties, presents on the system model – resulting of operating point variable and unmodeled dynamics – are adopted as control strategy the implementation of a digital Robust Model Reference Adaptive Controller (RMRAC). In this sense, the implementation of RMRAC controller are interesting to be showing robustness against unmodeled dynamics and parametric variations of plant, previously analyzed. The choice of reference model has as criteria the time of response and error on steady state. In this section are presented the design and structure of the adaptive control.

### *A. Structure of adaptive control*

For the implementation of adaptive control are necessary represented the system by means of a transfer function like:

$$G(s) = \frac{k \cdot Z(s)}{R(s)} \tag{8}$$

being Z(s) and R(s) are monic polynomials. However, since the transfer function (7) is a non-minimal phase system, to fit the small-signal model to the RMRAC controller design, the zero in the right half-plane of equation (7) will be considering an unmodulated dynamics. Therefore, the small-signal model will be represent as:

$$G_p(s) = G'_p(s) + \mu\Delta(s)\,, \tag{9}$$

$G'_p(s)$ represents the simplified small-signal model and $\mu\Delta(s)$ the unmodeled dynamics, involving for example the zero of $G_p(s)$. From analysis of (7), $G'_p(s)$ represented by:

$$G'_p(s) = \frac{V_{DC}(s)}{d(s)} = \frac{1.329 \cdot 10^{11}}{s^2 + 1.25 \cdot 10^4 s + 6.418 \cdot 10^7}\,. \tag{10}$$

To evaluate the validity of the model presented in (10), in Figure 7 the bode diagram of both models of small-signals is presented. Comparing the response of models, are possible verify that in the low frequencies both show similar behavior. As a reference model (RM), was chose a transfer function of relative degree 1, represented by:

$$W_m(s) = \frac{y_m(s)}{u(s)} = \frac{k_m \cdot Z_m(s)}{R_m(s)}\,, \tag{11}$$

where the parameters of reference model must be choice according the design requirements as the time of response, overshoot and error in steady state.

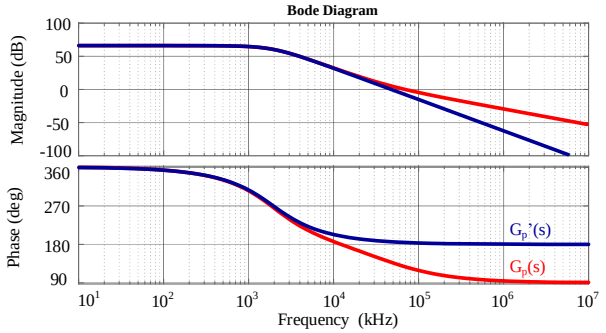


Fig. 7. Bode diagram of small-signal models $G_p(s)$ and $G'_p(s)$.

For the implementation of adaptive controllers has be chose as control strategy the use of gradient algorithm, due this structure showing a reduced number of interactions when compared with LS algorithms. This characteristic are interesting for the implementation of this system in DSP. Therefore, the control action u(*k*) must be calculated as follow: $u(k) = \theta^T(k) \cdot \omega(k)$, where $\theta(k)$ control gains vector to be adapted, given by:

$$\theta(k) = \left(\theta_1^T(k); \theta_2^T(k); \theta_y^T(k); \theta_r^T(k)\right)^T, \tag{12}$$

and $\omega(k)$ is $\omega(k) = [\omega_1^T(k); \omega_2^T(k); y(k); r(k)]^T$ [24].

$\omega(k)$ are updating has follow:

$$\begin{aligned} \omega_1(k+1) &= (\mathbf{I} + \mathbf{F} \cdot T_s) \cdot \omega_1(k) + \mathbf{q} \cdot T_s \cdot u(k), \\ \omega_2(k+1) &= (\mathbf{I} + \mathbf{F} \cdot T_s) \cdot \omega_2(k) + \mathbf{q} \cdot T_s \cdot y(k), \end{aligned} \tag{13}$$

where pair (**F**,**q**) are controllable with dimensions directly dependent on the relative order of the system. They must be chosen so that the filter given by $(s \cdot \mathbf{I} - \mathbf{F})^{-1}\mathbf{q}$ results in gains of 0 dB at the low frequencies of the signal of interest.

For the implementation of adaption law, the following recurrence equation it was adopt:

$$\theta(k+1) = \theta(k) - T_s \cdot \mathbf{\Gamma} \cdot \omega(k) \cdot \varepsilon_1(k) \cdot sgn(k_p/k_m)\,; \tag{14}$$

- $sgn(\cdot)$: are the signal function;
- $\varepsilon_1$ : augmented error, given by (16);
- $T_s$: sampling period;
- $\mathbf{\Gamma}$: matrix of adaptive gains;

$$\varepsilon_1 = y(k) - y_m(k) + \theta^T(k) \cdot \zeta(k) - W_m(z) \cdot \theta^T(k) \cdot \omega(k)\,; \tag{15}$$

In order to guarantee the robustness of the system the function $m^2$ is chose as normalization of the adaptive law: $m^2 = 1 + \omega^T \cdot \omega$. The parametric adaptation algorithm follows the block diagram presented in Figure 8, organized as follows:

1. Sampling of the system output: DC link voltage;
2. Updating of the reference signal;
3. Updating of the reference model;
4. Updating of the error signal: $e_1 = y(k) - y_m(k)$;
5. Updating of the augmented error;
6. Updating of the control gains vector: $\theta(k+1)$;
7. Updating of the matrix $\omega(k)$;
8. Updating of the control action: $u(k)$;
9. Updating of the adaptive law $m^2$;

*B. Design of controller*

Given the equation presented in the previous subsection, one must choose the reference models, and matrix **Γ** for the implementation of the closed-loop system. As sampling frequency, the switching frequency of the converter (20 kHz) it was used, in the way a sampling and an update of the gains to be adapted are carried out each cycle of operation.

For the regulation of DC link was defined as design criteria the time of response equal to 15 ms, due to the need to control the DC link voltage with a fast transient response, with no overshoot or error in steady state. For this, the reference model chosen was:

$$W_m(z) = \frac{0.006}{z - 0.994}. \qquad (16)$$

According to the chosen reference model, the parameters for the RMRAC controller implementation are summarized in Table II. The matrix Γ was chosen to result in a $\omega(k) = [\omega_1^T(k); \omega_2^T(k); y(k); r(k)]^T$ rapid and smooth transient response, in order to avoid overshoot during the adaptation of controller gains.

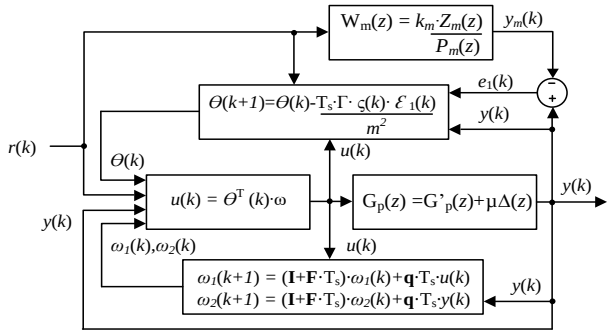


Fig. 8. Block diagram of adaptive controller.

**TABLE II**
**PARAMETERS AND INITIAL CONDITIONS OF THE RMRAC CONTROLLER**

| Symbol | Parameter | Values |
|---|---|---|
| θ | Adaptive gains | [ 0 0 0 0 ] |
| $\omega$ | Auxiliary vector | [ 0 0 0 0 ] |
| $T_s$ | Sampling period | 20 µs |
| F | Design parameter | -1 |
| q | Design parameter | 1 |
| Γ | Adaptive rate | 5·**I** |
| $W_m(z)$ | Reference Model | $W_m(z) = \frac{0.006}{z - 0.994}$ |

The results present in Figure 9 shows that both systems - closed-loop small-signal model and the reference model – have similar responses. The same test was be realized on power circuit of bidirectional converter, simulated using the PSIM to verify the response of RMAC controller to the unmodulated dynamic of the system. The response presented by Figure 10. In this result, we find certain differences in the values of the adapted gains, when compared with the Matlab simulated values. However, it is possible to verify that again the controller is able to follow the reference model according to the different voltage values of DC link.

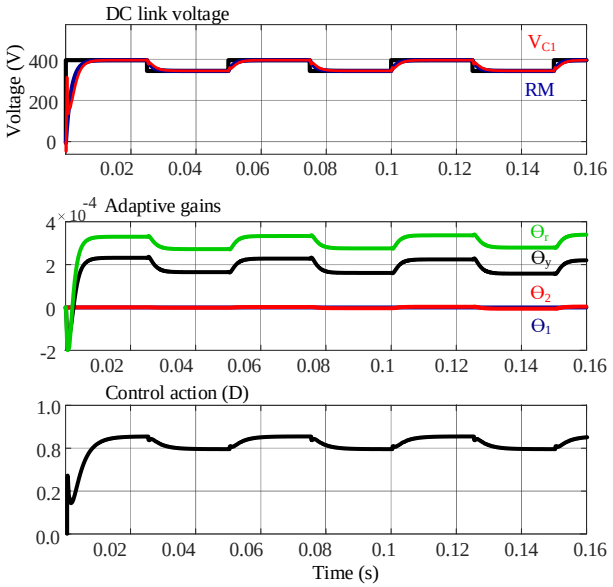


Fig. 9. Control of the converter simplified model $G_p(s)$ at closed-loop – Matlab.

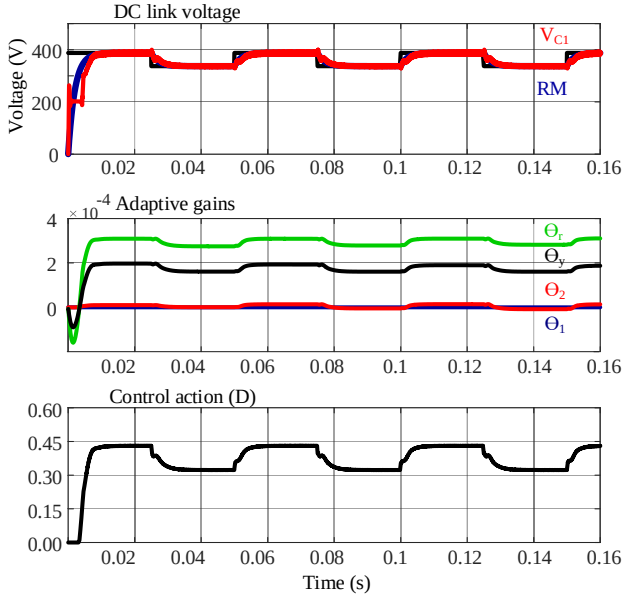


Fig. 10. Transient response of the DC link voltage for different reference values - PSIM.

At a last moment, the converter was tested with the objective to verify the capacity of RMRAC controller to regulate the DC link voltage, against variations of loads ($R_O$). In this test, power steps were applied to the DC link, varying between 50% and 100% of the rated power of the converter. From the result present in Figure 11, again is possible to verify the capacity of adaptive controller to regulate the DC link voltage, even with parametric variations such as changes in operating point and non-linearity of converter, represented by a linearized model. This result is of great interest for this work due to verification of the robustness of the system, especially for the regulation of the DC link voltage - due to the non-linearity of current-fed converter. This feature considerably limits the application of fixed gain controllers, for example PI or PID controllers, because when designed for a given operating point, they do not guarantee good performance outside the linear range of operation, for which they were designed.

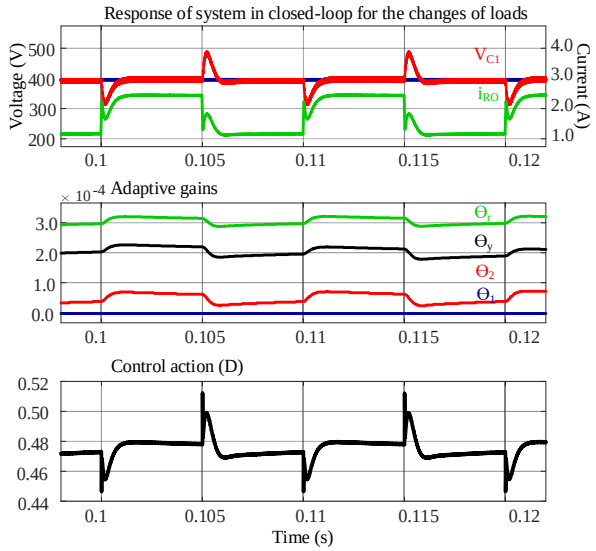


Fig. 11. Response of DC link regulation - PSIM.

## IV. Conclusions

The results obtained with the RMRAC controller proposed for the control of the discharge mode of a battery bank, from a bidirectional isolated converter, demonstrate high performance and robustness against parametric variations of the plant, adding reliability to the system, developed for applications in energy storage systems and regulation of DC links.

For the development of this work, the average model in state space was used to model the converter through the analysis of small-signals. However, due to the parametric variations involved in this type of system, the application of RMRAC controllers is justified, mainly, by the robustness presented to load variations and unmodulated dynamics. It is worth mentioning that the application of adaptive controllers has proven interesting for such application, since similar performance cannot be guaranteed with fixed-gain controllers.

Therefore, the proposed system presents as advantages: i) easy implementation in DSP by presenting a small number of interactions; ii) robustness to load variations; iii) independence of errors in small-signal models; iv) compensation of unmodulated dynamics and parametric variations. For future work, it is expected the implementation of the controller in DSP, as well as experimental results to corroborate with the presented analysis.

## Acknowledgments

The authors thank INCTGD, CAPES, CNPq, and FAPERGS for the financial support received for the development of this work. L. Michels were supported by a research grant of CNPq – Brasil. The present work was carried out with the support of the INCTGD and the financing agencies (CNPq process 465640/2014-1, CAPES process No. 23038.000776/2017-54 and FAPERGS 17/2551-0000517-1) and CAPES-PROEX. This study was financed in part by the Coordenação de Aperfeiçoamento de Pessoal de Nível Superior - Brasil (CAPES) - Finance Code 001.

## References

[1] Y. Wang, L. Xue, C. Wang, P. Wang, W. Li, “Interleaved High-Conversion-Ratio Bidirectional DC–DC Converter for Distributed Energy-Storage Systems-Circuit Generation, Analysis, and Design” IEEE Transaction on Power Electronics, Vol. 31, No. 8, 2016.

[2] M. H. Rashid, “Power Electronics Handbook: devices, circuits and applications handbook” 3ª Ed. Elsevier – Oxford, 2011.

[3] P. M. Curtis, “UPS Systems: Applications and Maintenance with an Overview of Green Technologies” Wiley-IEEE Pres, 1ª Ed. 2011.

[4] D. Linden, T. B. Reddy, “Handbook Of Batteries” 4ª ed. McGraw-Hill Professional, New York, 2011.

[5] A. Luque, S. Hegedus “Handbook of Photovoltaic Science and Engineering” Jhon Wiley & Sons Ltd, West Sussex, England, 2003.

[6] CBS Battery “VRLA Battery Characteristics” Taipei City, 2018.

[7] I. Barbi, M. Denizar, “Conversores Não-Isolados. Edição dos Autores, 6ª ed, Florianópolis, 2006.

[8] T. Wu, J. Yang, C. Kuo, Y. Wu, “Soft-Switching Bidirectional Isolated Full-Bridge Converter with Active and Passive Snubbers” IEEE Transactions on Industrial Electronics, Vol. 61, No. 3, 2014.

[9] H. Wen, W. Xiao, B. Su, “Nonactive Power Loss Minimization in a Bidirectional Isolated DC–DC Converter for Distributed Power Systems” IEEE Transactions on Industrial Electronics, Vol. 61, No. 12, 2014.

[10] H. Akagi, N. M. L. Tan, S. Kinouchi, Y. Miyazaki, M. Koyama, “Power-Loss Breakdown of a 750-V 100-kW 20-kHz Bidirectional Isolated DC–DC Converter Using SiC-MOSFET/SBD Dual Modules” IEEE Transactions On Industry Applications, Vol. 51, No. 1, p. 420-428, 2015.

[11] H. Wen, W. Xiao, B. Su, “Nonactive Power Loss Minimization in a Bidirectional Isolated DC–DC Converter for Distributed Power Systems” IEEE Transactions on Industrial Electronics, Vol. 61, No. 12, 2014.

[12] N. M. L. Tan, T. Abe, H. Akagi, “Design and Performance of a Bidirectional Isolated DC-DC Converter for a Battery Energy Storage System”, IEEE Transactions on Power Electronics, Vol. 27, no. 3, p. 1237-1248, 2012.

[13] E. Carvalho, E. Carati, J. P. Costa, C. M. O. Stein, R. Cardoso “Development of an Isolated Bidirectional Converter Applied on Charging and Discharging of Batteries Banks” Rev. Eletron. De Pot. – SOBRAEP, Vol. No. 2018.

[14] E. Carvalho, E. Carati, J. P. Costa, C. M. O. Stein, R. Cardoso “Design and Analysis of a Bidirectional Battery Charger” 8th Symposium on Power Electronics and Distributed Generation Systems, Florianópolis – 2017.

[15] E. Carvalho, E. Carati, J. P. Costa, C. M. O. Stein, R. Cardoso “Analysis, Design and Implementation of an Isolated Full-Bridge Converter for Battery Charging” 14th Brazilian Power Electronics Conference, Juiz de Fora – 2017.

[16] E. Carvalho, “Desenvolvimento de um Conversor Bidirecional Isolado para Controle de Carga e Descarga de Bancos de Baterias” master thesis, Universidade Tecnológica Federal do Paraná, Pato Branco, 2018.

[17] J. Zhang, S. Ci, H. Sharif, M. Alahmad, “Modeling Discharge Behavior of Multicell Battery” IEEE Transactions on Energy Conversion, Vol. 25, No. 4, 2010.

[18] J. Yang, B.Xia, Y. Shang, W. Huang, C. C. Mi, “Adaptive State-of-Charge Estimation Based on a Split Battery Model for Electric Vehicle Applications” IEEE Transactions on Vehicular Technology, Vol. 66, No. 12, 2017.

[19] C. Zou, C. Manzie, D. Nesic, “Model Predictive Control for Lithium-Ion Battery Optimal Charging” IEEE/ASME Transactions on Mechatronics, Vol. 23, No. 2, 2018.

[20] B. Zhao, Q. Song, W. Liu, Y. Su, “Overview of Dual-Active-Bridge Isolated Bidirectional DC–DC Converter for High-Frequency-Link Power-Conversion System” IEEE Transactions on Power Electronics, Vol. 29, No. 8, 2014.

[21] C. Zhao S.D. Round J.W. Kolar, “Full-order averaging modelling of zero-voltage-switching phase-shift bidirectional DC–DC converters” IET Power Electronics, Vol. 3, Iss. 3, 2010.

[22] H. Qin, J. W. Kimball, “Generalized Average Modeling of Dual Active Bridge DC–DC Converter” IEEE Transactions on Power Electronics, Vol. 27, No. 4, 2012.

[23] R. W. Erikson, D. Maksimovic, “Fundamental of Power Electronics” Kluwer Academic/Plenum Publishers, 2ª ed.- Boulder, Colorado. 2001.

[24] P. A. Ioannou; J. Sun, “Robust Adaptive Control”, [S.l.: s.n.], 1996.